

# SELECTION OF HEAT TREATMENT PARAMETERS FOR A CAST ALLVAC 718Plus® ALLOY

Oscar Caballero<sup>1</sup>, Kepa Celaya<sup>1</sup>, Tomás Gomez-Acebo<sup>2</sup>, Antonio Julio Lopez<sup>2</sup>

<sup>1</sup>ITP, Industria de Turbo Propulsores, S.A.

Edificio no. 300, Parque Tecnológico, 48170 Zamudio, Vizcaya, Spain

<sup>2</sup>CEIT Centro de Estudios e Investigaciones Técnicas

Paseo Manuel Lardizabal, 15, 20009 San Sebastián, Guipuzcoa, Spain

Keywords: 718Plus, casting, heat treatment, VITAL R&D

## Abstract

The first selection of best set of parameters for heat treating a cast Allvac 718Plus alloy is presented in this paper. The high interest from several aeroengine manufacturers in this new alloy with improved temperature capabilities over widely used In718 has driven the development of the alloy also in the direction of making available a cast form of it. A first step in this direction was to use some available material (billet originally intended to be used for forging other parts) as remelting stock for producing a couple of cast rings and use them as test material for assessment of different sets of heat treatment parameters. In particular, the application of homogenization before HIP and the solution temperature after HIP are discussed. Use of hardness measurements and optical microscopy were made to help in the assessment of the effect of the homogenization cycle, and also the effect of the different solution temperatures. Other techniques such as Scanning Electron Microscope and X-Ray Diffraction were tried for identification and quantification of hardening phases.

## Introduction

Alloy Allvac 718Plus has been marketed by its inventor, Dr W.D. Cao, and producer company, Allvac, and several articles have been published or fostered from the company to show the advantages over the widely used In718 [1, 2, 3]. The new alloy claims to offer better mechanical properties at those temperatures where In718 has already exhausted its applicability, in the 650°C range. Allvac 718Plus shows improved metallurgical stability at even higher temperatures, up to 700°C. In this upper range, no degradation of mechanical properties has been noticed for the new alloy [4].

The alloy was originally developed to be used in its wrought form, but requests from aeroengine companies have driven Allvac to perform activities in order to tune-up the chemical composition of the alloy in its cast form and also trim the heat treatment of this application. This paper shows one of the first efforts to select the heat treatment to be applied to this kind of material.

ITP and CEIT were partners in the European VITAL R&D program, together with Volvo Aero Corporation, where several activities were performed to evaluate the new alloy. One of these was the production of castings in different geometries, such as separately cast test bars, stair shaped plates, hollow rings and a demonstration casting to finally assess castability [5]. The present study consisted of heat treatment trials and mechanical property assessments of cast rings. This paper covers the heat treatment studies.

## Experimental Procedure

Several cast Allvac 718Plus solid rings were produced at PCB, Baracaldo, Spain, by the conventional investment casting. Dimensions of the rings were 285 mm OD, 225 mm ID, and 120 mm high. See Figure 1.



Figure 1. Cast Allvac 718Plus rings produced at PCB.

The remelt stock used for production of these rings was originally intended to be used as forging stock. The chemical composition of the material was that of the billet produced for the VITAL project, used as remelting stock, given in Table 1:

C	Mn	Si	Cr	Mo	Co	Ti	Al	B	Zr	Fe	P	Nb	W	V	Nickel
0.19	0.04	0.04	17.8	2.67	9.0	0.75	1.43	0.004	<0.01	9.5	0.01	5.5	1.0	0.02	Bal.

Table 1: Chemical composition of 718Plus alloy for production of cast rings, weight percent.

After completing their initial NDT evaluation, several heat treatments were applied to different samples from the rings, as described in Table 2 to study the use of homogenization prior to HIP, and solution temperatures from 954°C to 1066°C after HIP.

Details of the first steps of heat treatment sequence were as follow:

Ring 1 was homogenized at 1095°C for 1 hour, and cooled at 2 bar of Ar pressure.

Both rings were HIPed at 1120°C, in Ar gas at 103 MPa for 4 hours.

The rings were then cut and the different samples underwent solution heat treatments at different temperatures, as described in Table 2. After these solution heat treatments, samples were aged at the usual Allvac 718Plus parameters: 788°C during 8 hours, cool to 704°C, hold during 8 hours, cool to room temperature.

Finally, the samples received a simulated service treatment of 700°C for 140 hours followed by 675°C for 460 hours. This simulated cycle represents the most severe conditions that the Allvac cast 718Plus components might be expected to see. These conditions would preclude the use of In718 due to thermal degradation of the material. Only the upper temperature range service conditions were simulated. Table 2 shows the whole set of produced samples. HHX is the

reference for Homogenised and HIPed sample number X, and NHY is the reference for the only HIPed sample number Y.

Solution Temperature	As produced (after HIP)	Solutioned	Aged	Exposed
Without solution	HH0/NH0	Not applied	Not applied	Not applied
954°C	N/A	HH1/NH1	HH6/NH6	HH11/NH11
982°C	N/A	HH2/NH2	HH7/NH7	HH12/NH12
1010°C	N/A	HH3/NH3	HH8/NH8	HH13/NH13
1038°C	N/A	HH4/NH4	HH9/NH9	HH14/NH14
1066°C	N/A	HH5/NH5	HH10/NH10	HH15/NH15

Table 2: Set of samples investigated, with different solution heat treatment temperatures and addition of HIP.

Hardness testing and microstructural observations were used to assess the results of the different applied heat treatments. Rockwell C and Vickers measurements were used initially to assess macroscopic and microscopic features of the heat treated material. As the scatter of the obtained values was outside the valid range in some of the samples, it was afterwards decided to use the Brinell scale to allow for comparisons amongst all the different samples.

### Results

The values obtained from the Brinell hardness measurements are shown in Table 3. Each value is an average of measurements taken at five different points.

Heat Treat Parameters	Brinell Hardness, HB			
	As produced (after HIP)	Solutioned	Aged	Exposed
Hom, HIP	HH0 302			
Hom, HIP, 954°C	N/A	HH1 251	HH6 379	HH11 367
Hom, HIP, 982°C	N/A	HH2 256	HH7 356	HH12 364
Hom, HIP, 1010°C	N/A	HH3 226	HH8 364	HH13 373
Hom, HIP, 1038°C	N/A	HH4 217	HH9 351	HH14 389
Hom, HIP, 1066°C	N/A	HH5 218	HH10 371	HH15 413
HIP	NH0 310			
HIP, 954°C	N/A	NH1 257	NH6 365	NH11 362
HIP, 982°C	N/A	NH2 261	NH7 358	NH12 369
HIP, 1010°C	N/A	NH3 213	NH8 353	NH13 377
HIP, 1038°C	N/A	NH4 227	NH9 363	NH14 373
HIP, 1066°C	N/A	NH5 221	NH10 373	NH15 383

Table 3: Brinell hardness values of the samples obtained after heat treatment trials.

The values are plotted in Figures 2 and 3.

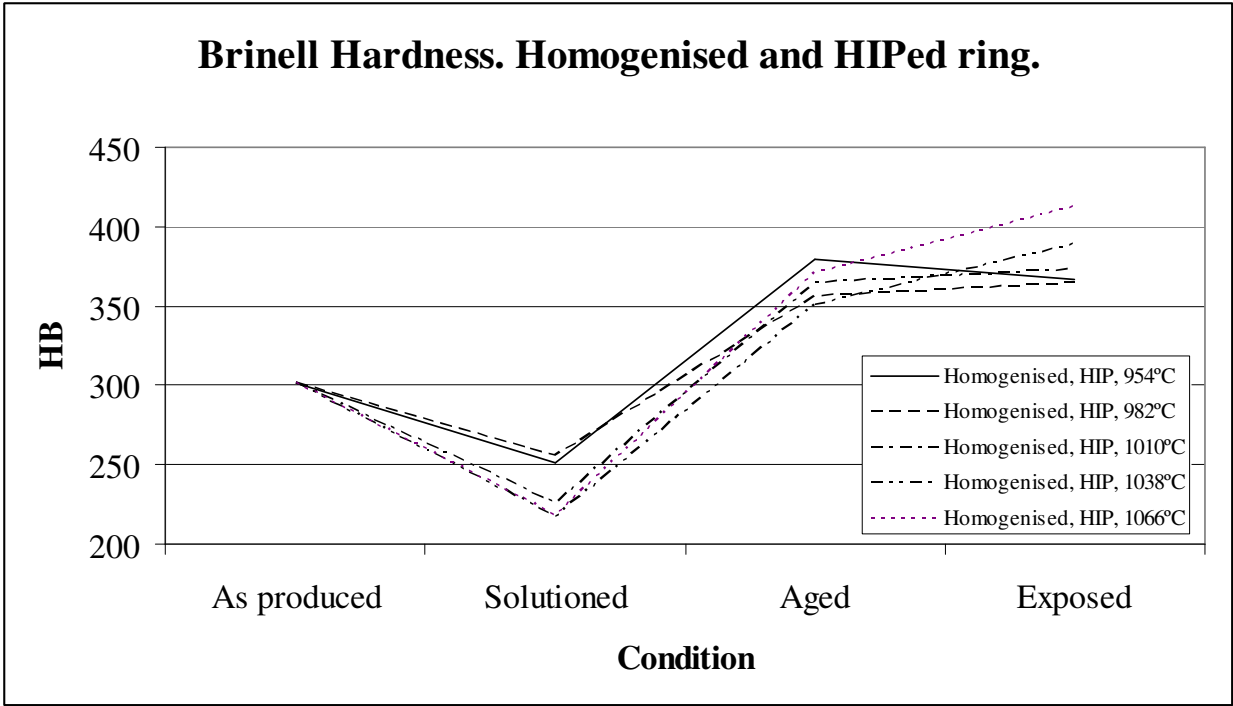


Figure 2: Average values of Brinell hardness on metallographic examples from Homogenized and HIPed ring with different solution temperatures.

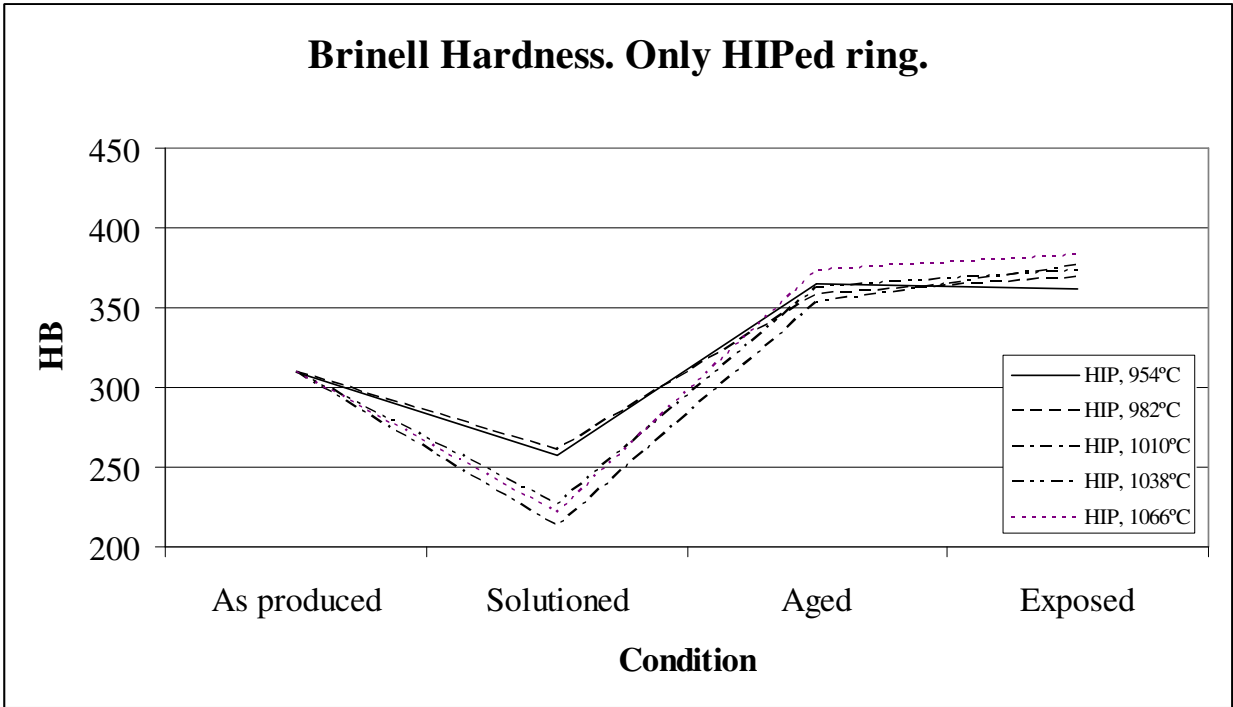


Figure 3: Average values of Brinell hardness on metallographic examples from only HIPed ring with different solution temperatures.

Comparison between both sets of data shows that the hardness values of the homogenized samples increased after the simulated service exposure conditions, especially the samples that

were heat treated at higher solution temperatures. This is attributed to a larger amount of available Nb and other hardening elements in the matrix for forming precipitates, as the homogenization cycle has contributed to dissolve the segregations and place those elements into solution in the matrix. The homogenization heat treatment worked out satisfactorily in spite of being 1hr and 1095°C, that is shorter and at lower temperature than the HIP. In fact, measurements on samples revealed that Nb segregations percentages were always reduced by the homogenization cycle. Comparing Micrographs 1 versus 2, solutioned at one temperature, and Micrographs 3 versus 4, solutioned at another different temperature, the size and percentage of Nb segregations are larger in the only HIPed metallographic samples. On the homogenized metallographic samples, the phases are more evenly distributed. Measurements of volumetric fractions of Nb segregations were performed on micrographs of etched material that were analysed through Leica Qwin image analysis program. This effect of higher dissolution of the segregations (lower volumetric fraction) was confirmed, see Figure 4.

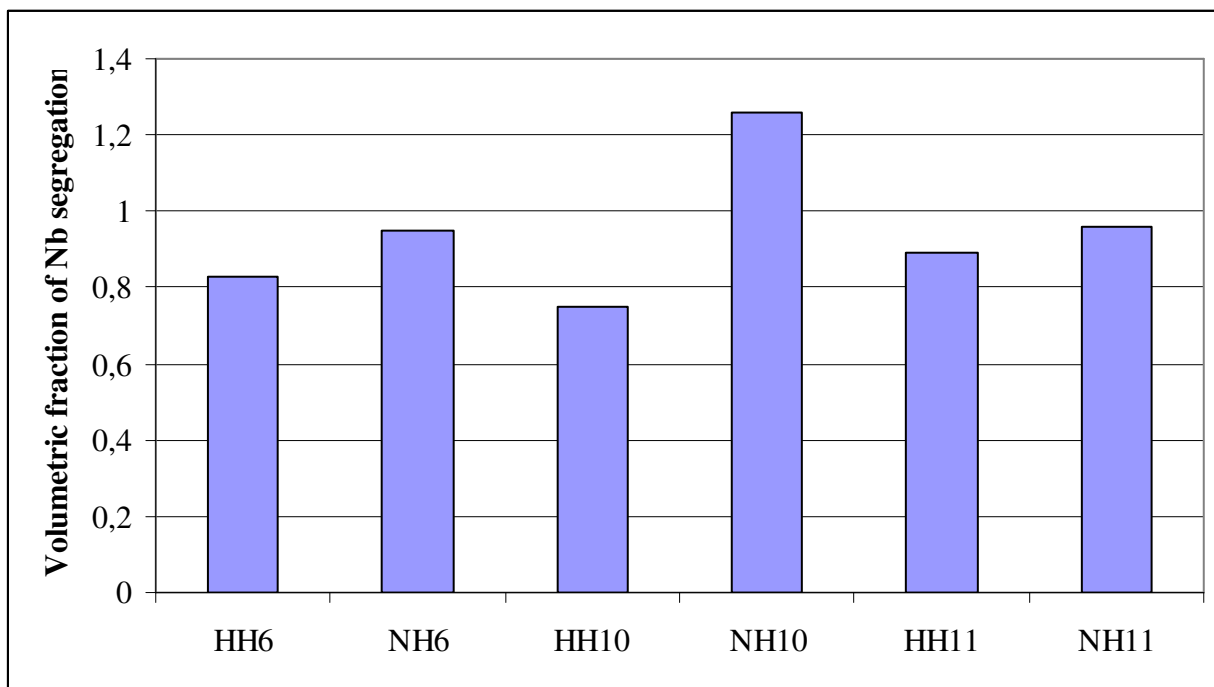
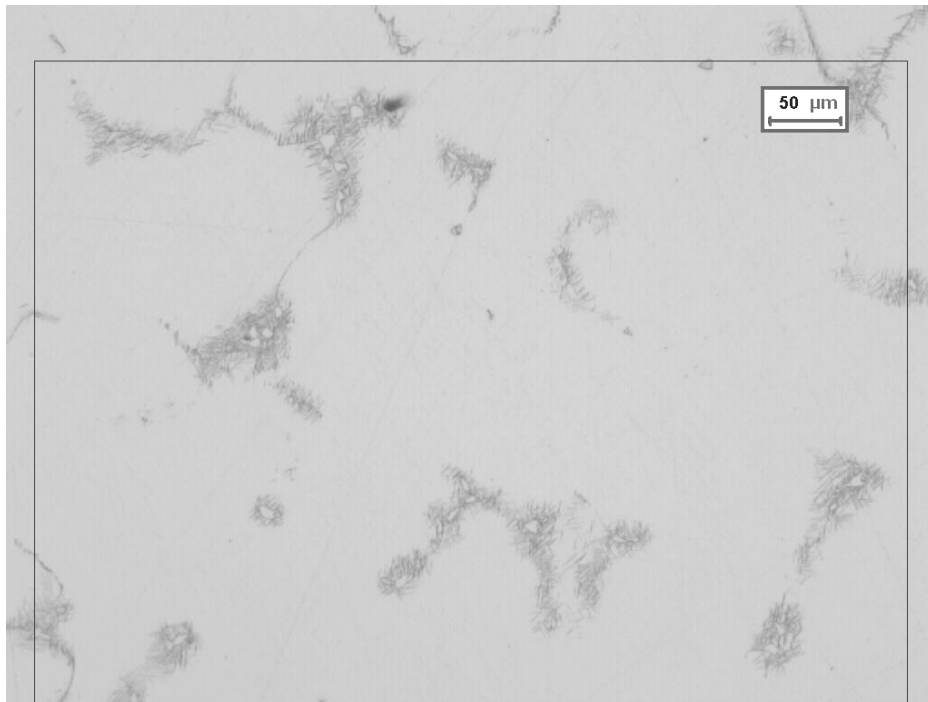
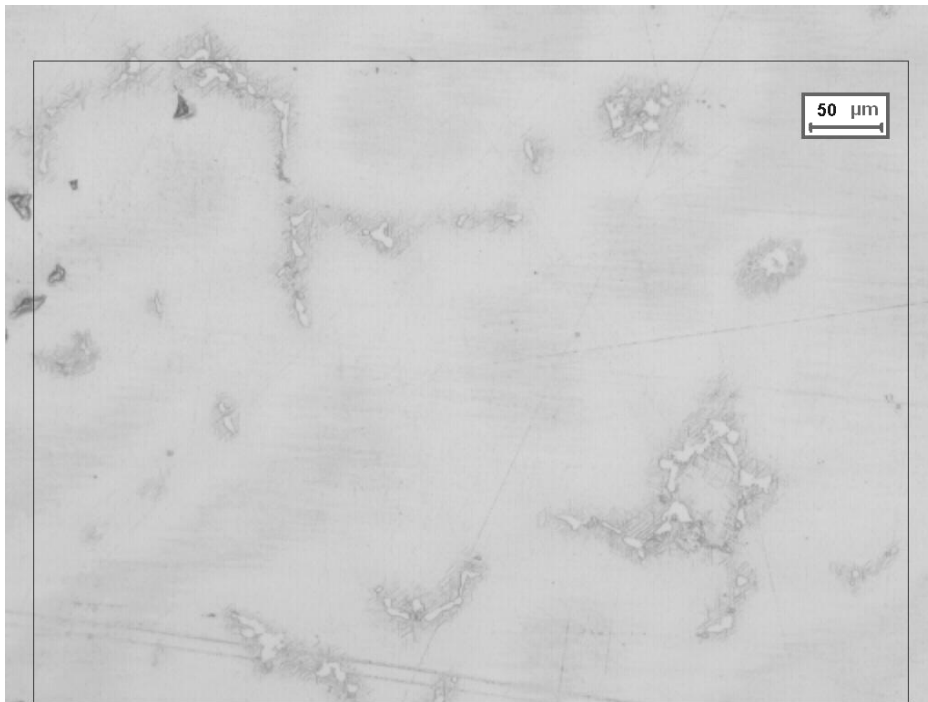


Figure 4. Volumetric fraction of Nb segregations in 718Plus cast samples after thermal treatments.

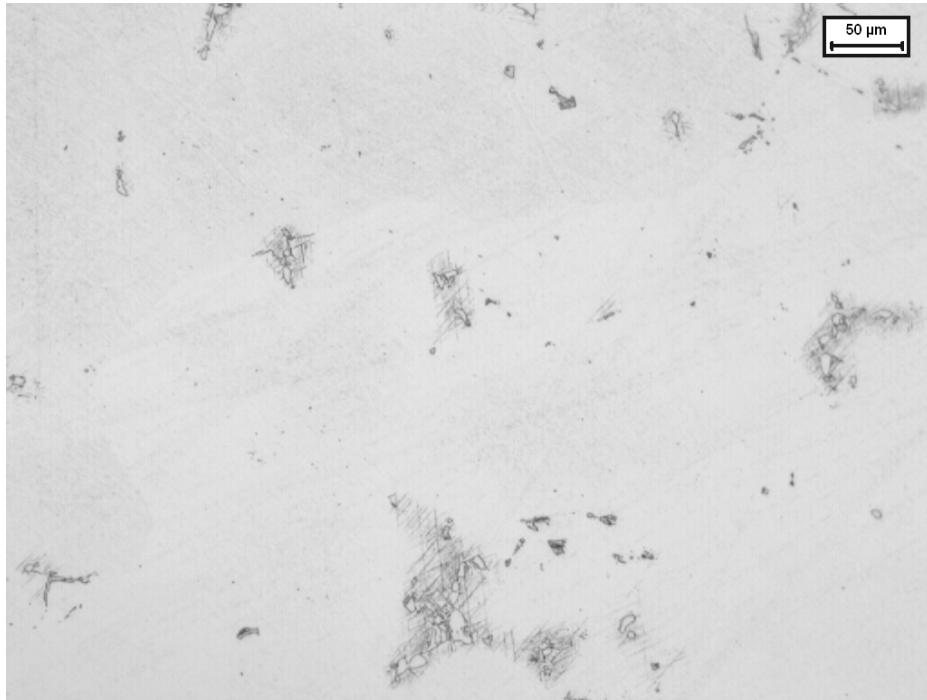
At the same time, the higher solution temperatures have also contributed to dissolve larger amounts of  $\delta$  phase, making more Nb and other hardening elements available for forming hardening phases. This can be observed when comparing Micrographs 1 and 2 to Micrographs 3 and 4, respectively. The  $\delta$  phases formed around Nb segregations extend more into the matrix when the solution temperature is lower. At higher solution temperatures, those  $\delta$  needles are dissolved and thus the Nb is free to form other hardening phases.



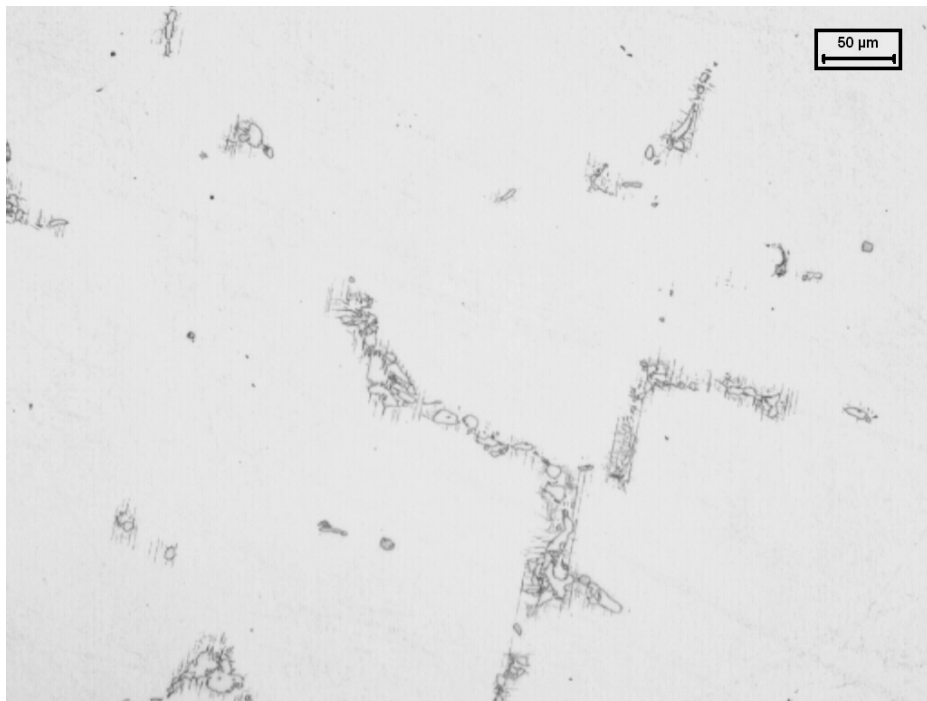
Micrograph 1: Metallographic sample HH1, solutioned at 954°C from Homogenized and HIPed ring.



Micrograph 2: Metallographic sample NH1, solutioned at 954°C from only HIPed ring.  
Larger Nb segregations (than those in Micrograph 1) can be observed.

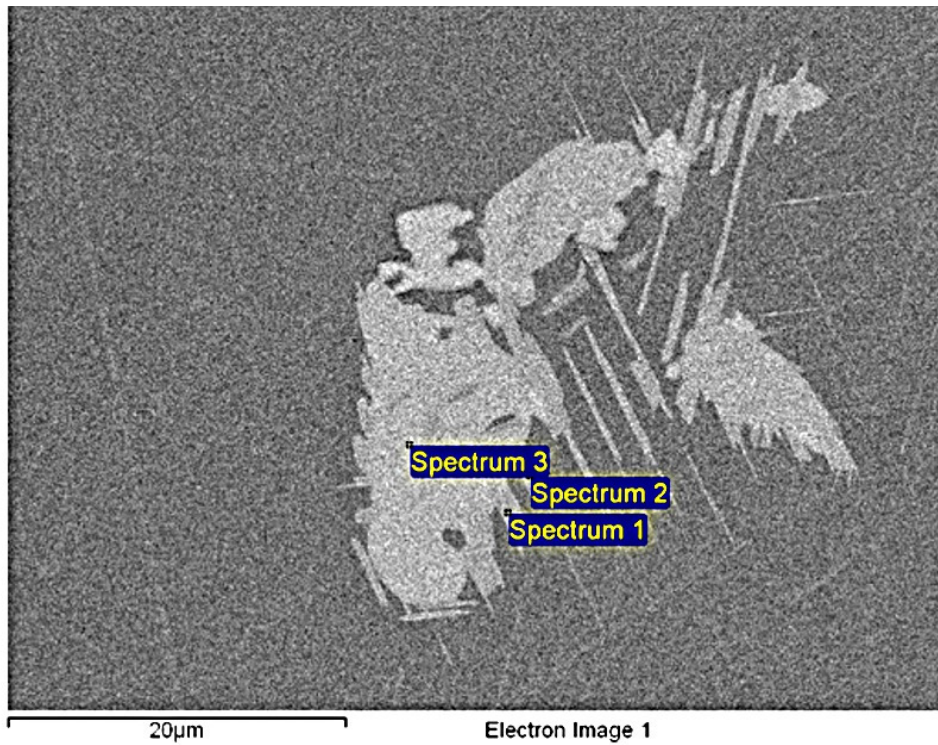


Micrograph 3: Metallographic sample HH5, solutioned at 1066°C from Homogenized and HIPed ring.

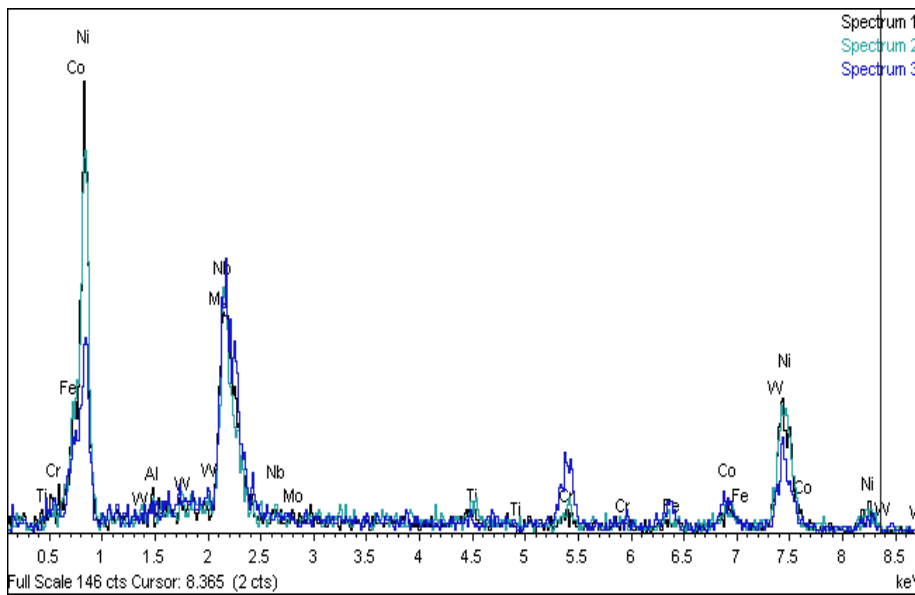


Micrograph 4: Metallographic sample NH5, solutioned at 1066°C, from only HIPed ring.

The blocky islands found in these micrographs were assumed to be segregations formed during the solidification process of these rather thick rings, with Nb retained in them. This was confirmed later on through EDAX analysis in the SEM, see Micrograph 5 and Table 4.



Micrograph 5: FEG-SEM (BSE) micrograph of NH5 sample (ST: 1066 °C)

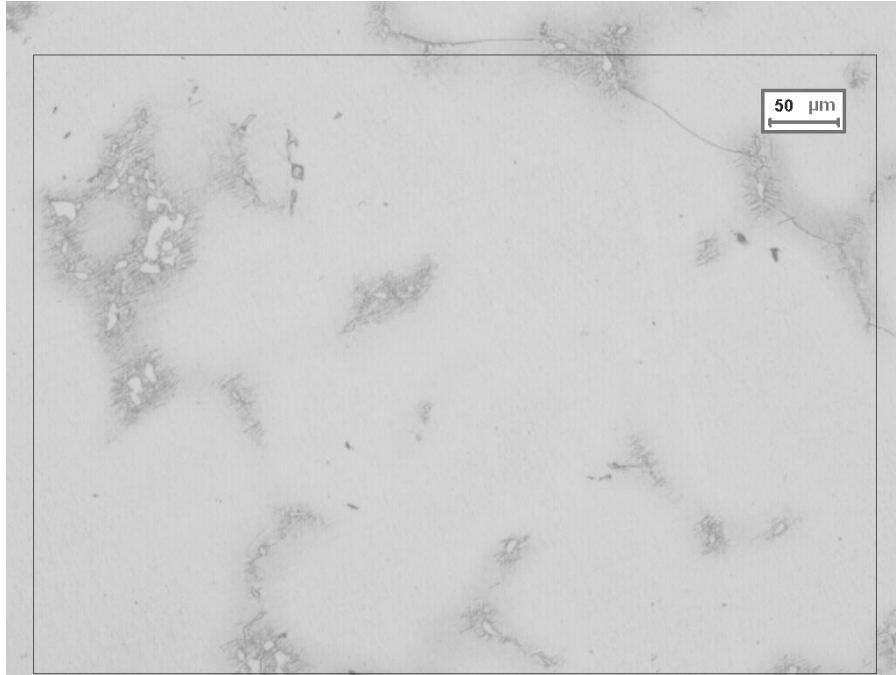


Spectrum	Al	Ti	Cr	Fe	Co	Ni	Nb	Mo	W
Spectrum 1	0.64	1.16	2.56	1.56	6.49	54.53	29.54	2.40	1.11
Spectrum 2	0.21	2.13	3.10	2.90	6.14	53.90	28.15	1.34	2.13
Spectrum 3	0.47	0.42	10.97	5.34	10.73	34.12	30.27	5.88	1.80

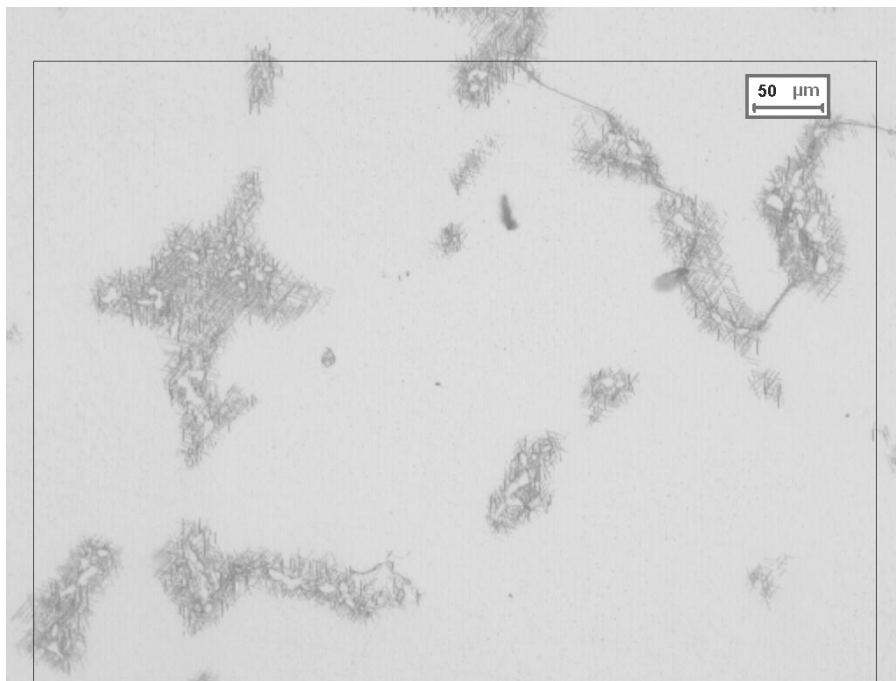
Table 4: EDS micro-analyses of marked zones at Micrograph 5.

## Discussion

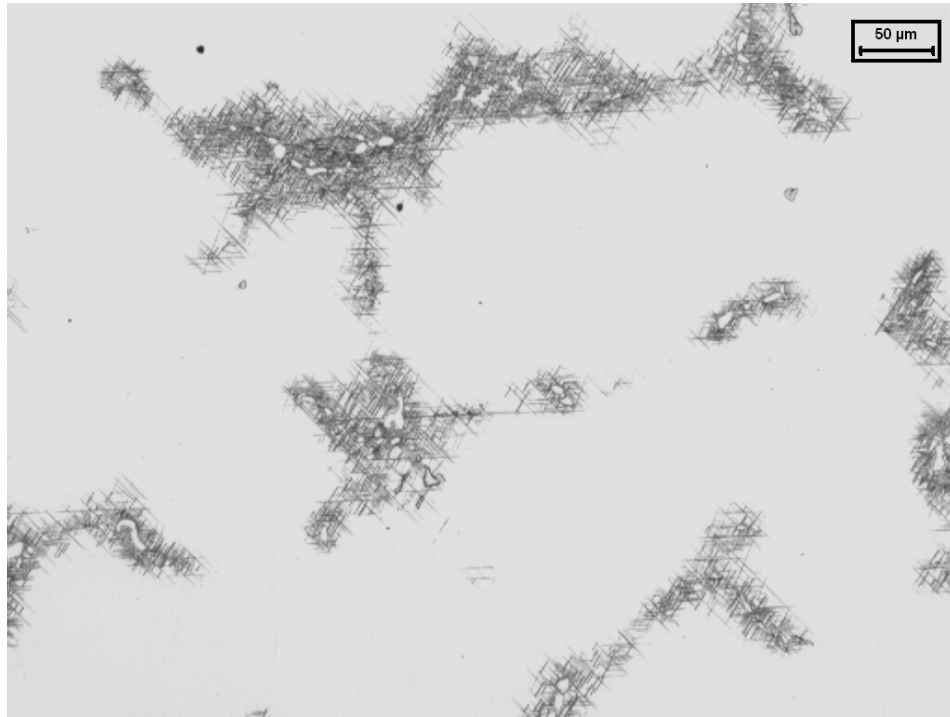
Clearly, on the 982°C and 1010°C solution micrographs, more precipitation of acicular  $\delta$  phase is observed than in the 954°C solution micrographs (darker areas in micrographs). Comparison of Micrographs 6, 7 and 8 shows this effect. The blocky islands, whiter zones surrounded by the  $\delta$  phase, were identified as Nb segregations, as explained earlier.



Micrograph 6 : Metallographic sample HH6, solutioned at 954°C and aged, from Homogenized and HIPed ring.



Micrograph 7: Metallographic sample HH7, solutioned at 982°C and aged, from Homogenized & HIPed ring.



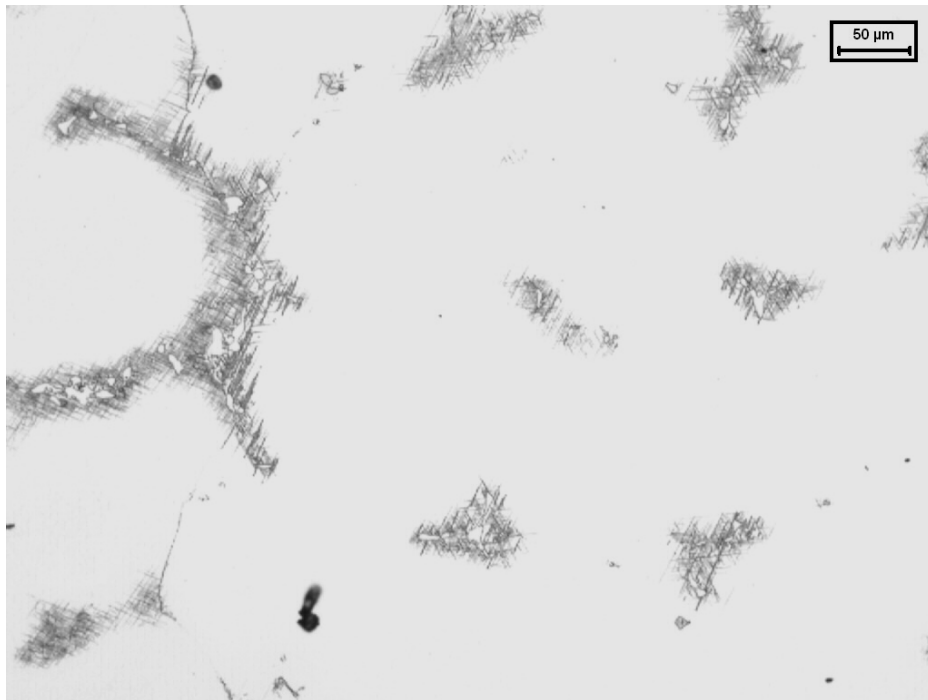
Micrograph 8: Metallographic sample HH8, solutioned at 1010°C and aged, from Homogenized & HIPed ring.

However, it is surprising that  $\delta$  phase is still present at 1038°C or 1066°C. This  $\delta$  phase should have been completely dissolved at these temperatures. See Micrographs 9 to 12.

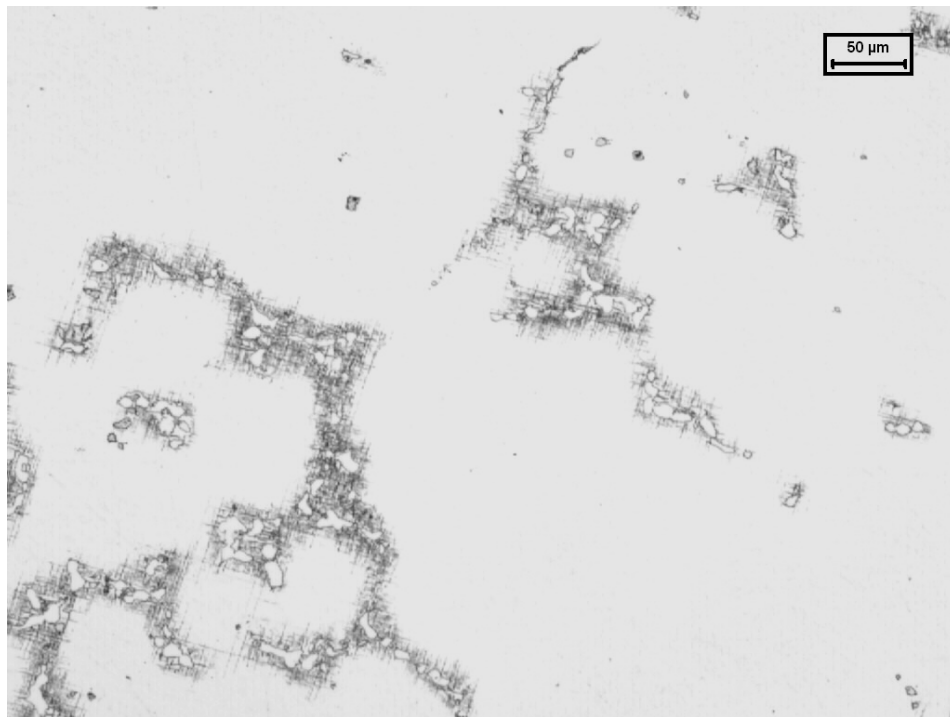
It is thought that the  $\delta$  phases are still present even after application of very high solution temperatures because they are surrounding the Nb segregation areas. For the same heat treatment condition, and throughout the different steps,  $\delta$  phase seems to continue to form from the prior as-cast Nb segregation. As the Nb dissolves during heat treatment, there is more Nb available to form  $\delta$  phase. Thus, both the volume fraction and size of acicular  $\delta$  phase increases as heat treatment progresses through its steps.

The volume fraction and size of acicular delta phase and Nb segregated areas are also observed to depend on what solution temperature is applied.  $\delta$  phase volume fraction seems to be maximum when the solution temperature is 982°C, but decreases again with higher solution temperatures.  $\delta$  phase starts to solve when the temperature is above 1000°C, which is known to be the range of  $\delta$  solvus.

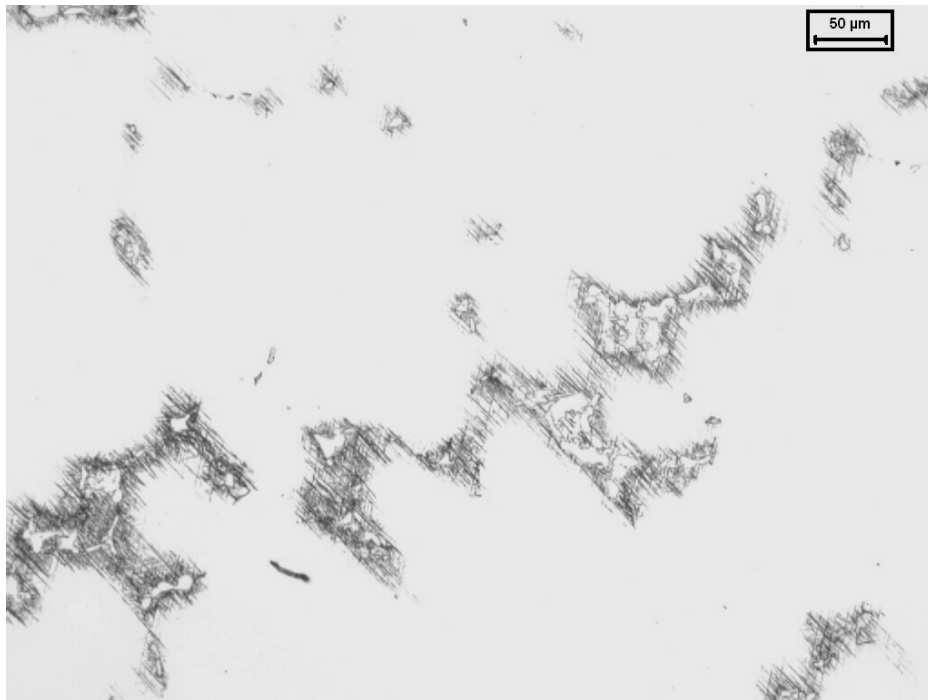
As there is always a transition area between the Nb segregation and the matrix, the  $\delta$  still appears there, but the higher solution temperatures cause these  $\delta$  phase needles to get into solution quicker when they pass through these temperatures, making more hardening elements available to form precipitates, which are not visible in the optical microscope. This reasoning is consistent with hardness values measured in the exposed condition.



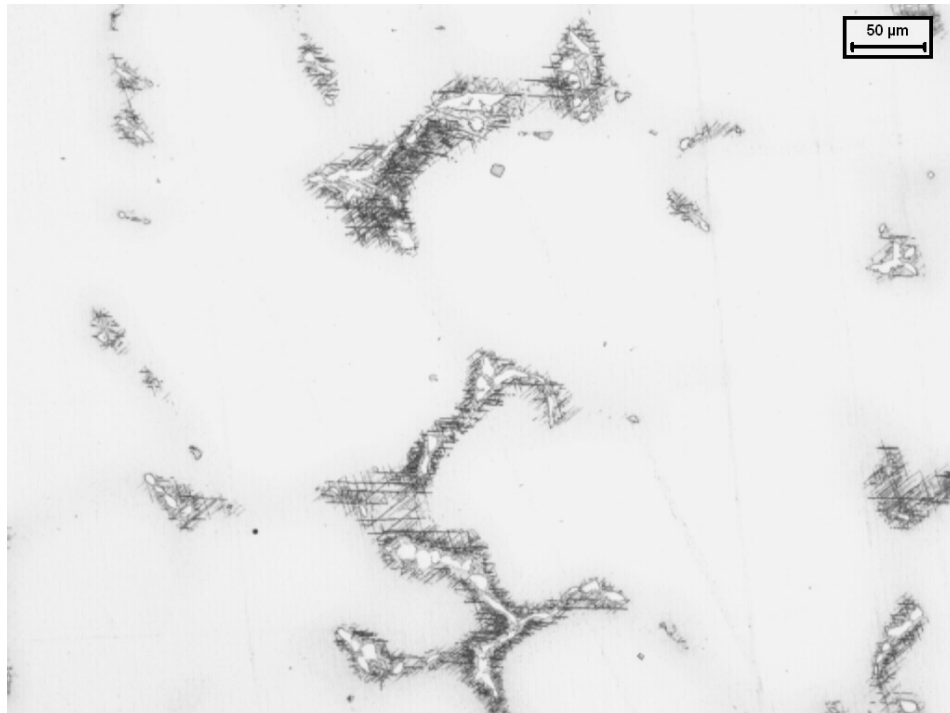
Micrograph 9: Metallographic sample HH9, solutioned at 1038°C and aged, from Homogenized & HIPed ring.



Micrograph 10: Metallographic sample HH10, solutioned at 1066°C and aged, from Homogenized & HIPed ring.



Micrograph 11: Metallographic sample NH9, solutioned at 1038°C and aged, from only HIPed ring.



Micrograph 12: Metallographic sample NH10, solutioned at 1066°C and aged, from only HIPed ring.

In order to assess the effect of thermal exposure on the material,  $\gamma'$  phase sizes were also measured. Table 5 shows some of these sizes to illustrate the growth of these precipitates. This particular case shows that the growth of  $\gamma'$  phase is related with a decrease in the hardness values, but this is almost the only case in which this happens. A possible rationale for the increase of the hardness values at the rest of the solution temperatures is that these higher solution temperatures achieved an effective solution of  $\delta$ , making more Nb available to form other hardening phases, such as  $\gamma''$ , and this was the one responsible for the increase in hardness values. However, it is difficult to admit this, as the alloy is known to be primarily hardened by  $\gamma'$ , and not by  $\gamma''$ .

Sample	Average diameter or length of $\gamma'$ (nm)	Standard deviation (nm)
NH6	110	10
HH11	140	20
NH11	140	10

Table 5. Average size and standard deviation of  $\gamma'$  precipitates, for the different samples.

It is also observed that the sizes of the precipitates do not change regardless the previous application or not of homogenization heat treatment. This indicates that homogenisation only dissolves segregations to make more hardening elements available, but doesn't really have any effect on the size or morphology of precipitates formed later in the heat treatment.

Finally, after all observations, 982°C was selected as the solution temperature, which is at the upper end of the wrought material AMS specification range for solution heat treatment. The volume fraction of acicular  $\delta$  phase is also higher than with the 954°C solution temperature, which is at the lower end of the same AMS specification. The hardness values, which give an indication of mechanical properties of the material condition, are higher than those obtained with the 954°C solution heat treatment.

Although the application of homogenization demonstrated a better distribution of hardening elements, the benefit was not judged to a significant improvement. As no deleterious effect was observed when homogenization was not employed, and bearing in mind the cost reduction associated to removal of this treatment, it was decided to only HIP the cast material.

Therefore, the remainder of the ring that had not received the homogenization heat treatment was selected for mechanical properties characterization, and the 982°C solution heat treatment was applied to this material. Results on these tests are detailed elsewhere [5].

## Conclusions

1. The 982°C and 1010°C solution treatments produced more precipitation of acicular  $\delta$  phase than the 954°C solutioning. Formation of  $\delta$  phase is promoted at these higher temperatures, as diffusion of Nb occurs from the as-cast Nb rich segregation areas.
2. Some  $\delta$  phase is still present after 1038°C, 1066°C solution treatments. This  $\delta$  should have been completely dissolved under equilibrium conditions at these temperatures. It is thought that it is still present because it is formed from the Nb segregation areas, as there is always a transition area between the Nb segregation and the matrix. In other words, precipitation of  $\delta$  phase is usually produced by overaging, but it also happens because of the diffusion of the Nb segregations during solution heat treatment.

3. On the only HIPed metallographic samples, the Nb segregations are bigger or present in higher quantity; percentage of present phase and phase-sizes are higher. The homogenization heat treatment worked out satisfactorily in spite of being 1hr and 1095°C, that is shorter and at lower temperature than the HIP.

4. Clear over-aging of samples solutioned at lower temperatures, has happened because of the thermal exposition treatment. This point has been observed not only by FEG-SEM images and measurements of the  $\gamma'$  size that reveals its coarsening, but also by hardness measurements. Higher solution temperatures change the sense of this effect. This could be attributed to the formation of additional  $\gamma''$  from Nb stemming from dissolution of segregations.

5. Previous homogenization treatment does not affect the size of  $\gamma'$  precipitates.

### References

1. "Allvac® 718Plus®, Superalloy for the Next Forty Years", R.L. Kennedy, Superalloys 718, 625, 706 and Various Derivatives, TMS, 2005.

2. "Role of Chemistry in 718-Type Alloys – Allvac® 718Plus® Alloy Development", W.D. Cao, R. Kennedy, Superalloys 2004.

3. "Developments in Wrought Nb Containing Superalloys (718+ 100 °F)", R.L. Kennedy, W.D. Cao, T.D. Bayha, R. Jeniski, TMS, 2003.

4. "Comparison between the Microstructure and the Mechanical Properties of In718 and 718Plus Alloys after Exposition" T. Gómez-Acebo, A.J. Lopez, J.C. Rodríguez, O. Caballero, M. Goiricelaya, K. Celaya, G. Sjoberg, M. Hörnqvist, Superalloy 718 symposium, Pittsburgh, October 2010.

5. "Overview on 718Plus assessment within VITAL project", O. Caballero; G. Sjoberg; T. Gómez-Acebo, Superalloy 718 symposium, Pittsburgh, October 2010.